Endocrine Journal 2025, 72 (5), 495-507. doi:10.1507/endocrj.EJ24-0505

ORIGINAL

Scutellarin mitigates high glucose-induced pyroptosis in diabetic atherosclerosis: Role of Nrf2-FBXL2-mediated NLRP3 degradation

Qingxin Meng[1], Yongpan Huang[1], Xian Long[1], Lijing Liu[1], Yani Tang[1], Jingjing He[1] and Yayuan Luo[2]

[1] *School of Medicine, Changsha Social Work College, Changsha, Hunan Province 410004, China*
[2] *Department of Neurology, Hunan Aerospace Hospital, Changsha, Hunan Province 410205, China*

Abstract. This study investigated the role of scutellarin (Scu) and Nrf2 in diabetic atherosclerosis, focusing on their effects on FBXL2 and NLRP3 ubiquitination. Human umbilical vein endothelial cells were treated with high glucose (HG) to model diabetic atherosclerosis *in vitro*. Cell viability, cytotoxicity, pyroptosis, and inflammatory cytokine levels were assessed, and gene interactions were examined by dual-luciferase reporter assays. Ubiquitination and protein levels were analyzed through immunoprecipitation and western blotting. The results revealed that HG treatment decreased Nrf2 and FBXL2 levels and enhanced NLRP3-mediated pyroptosis. However, Scu treatment increased Nrf2 expression, improved cell viability, and inhibited pyroptosis. Nrf2 knockdown downregulated FBXL2 and reversed the protective effects of Scu. Additionally, FBXL2 promoted the ubiquitination-mediated degradation of NLRP3 and suppressed pyroptosis. The activation of NLRP3 reversed the protective effects of Scu on diabetic atherosclerosis. These findings suggest that Scu alleviated diabetic atherosclerosis by increasing Nrf2 and FBXL2 expression, promoting NLRP3 ubiquitination-mediated degradation, and suppressing pyroptosis.

Key words: Diabetic atherosclerosis, Pyroptosis, Scutellarin, Nrf2, FBXL2

Introduction

Atherosclerosis, a chronic inflammatory disease, is a leading cause of cardiovascular morbidity and mortality worldwide [1, 2]. Individuals with diabetes face a substantially greater risk of developing coronary atherosclerotic heart disease than do those without diabetes [3]. The pathogenesis of atherosclerosis involves various mechanisms, including macrophage polarization, advanced glycation end products, insulin resistance, and dysregulation of the ubiquitin-proteasome system [4]. Endothelial cell pyroptosis plays a critical role in the development and progression of atherosclerosis in diabetic individuals [5]. Therefore, elucidating the molecular mechanisms underlying endothelial cell pyroptosis and exploring potential therapeutic interventions might be of significant scientific interest.

Scutellarin (Scu), a bioactive compound derived from the traditional Chinese medicinal plant *Erigeron breviscapus*, has shown promising effects in various cardiovascular conditions [6]. Oxidative stress, characterized by an imbalance between reactive oxygen species and antioxidant defenses, plays a critical role in the pathogenesis of cardiovascular diseases [7]. Previous studies have suggested that Scu inhibits oxidative stress, highlighting its potential role in mitigating diabetes-related cardiovascular diseases [8]. However, further research is needed to elucidate the precise mechanisms and therapeutic implications of Scu in the context of diabetic atherosclerosis.

Nuclear factor erythroid 2-related factor 2 (Nrf2) is a crucial transcription factor involved in the cellular defense against oxidative stress [9]. It regulates the expression of numerous antioxidant and detoxification genes, thereby maintaining redox homeostasis and protecting against cardiovascular diseases [10]. Nrf2 activation has been shown to enhance endothelial function and reduce the risk of chronic diseases associated with atherosclerosis [11]. Investigating the mechanisms through which Nrf2 influences endothelial dysfunction and delays the progression

Submitted Oct. 16, 2024; Accepted Dec. 30, 2024 as EJ24-0505
Released online in J-STAGE as advance publication Feb. 26, 2025
Correspondence to: Qingxin Meng, School of Medicine, Changsha Social Work College, No. 421, Xiangzhang Road, Yuhua District, Changsha, Hunan Province 410004, China.
E-mail: mindy09meng@163.com
Abbreviations: HG, high glucose; HRP, horseradish peroxidase; HUVECs, human umbilical vein endothelial cells; IP, immunoprecipitation; LDH, lactate dehydrogenase; ANOVA, one-way analysis of variance; PI, propidium iodide; NLRP3, NOD-like receptor family pyrin domain-containing protein 3; NC, negative control; Nrf2, nuclear factor erythroid 2-related factor 2; Scu, scutellarin

of atherosclerosis is highly important for the development of novel therapeutic strategies. Recent evidence suggests that Scu can increase Nrf2 expression [12], potentially conferring benefits for attenuating the progression of atherosclerosis.

FBXL2 is a member of the F-box protein family and is involved in the process of ubiquitination-mediated degradation [13]. Recent studies have shown that FBXL2 can ubiquitinate and degrade NOD-like receptor family pyrin domain-containing protein 3 (NLRP3), a key regulator of the inflammatory response [14, 15]. This degradation of NLRP3 influences macrophage pyroptosis, a form of cell death associated with inflammation [16]. However, the role of FBXL2 in endothelial cells and its potential involvement in atherosclerosis remain largely unexplored.

On the basis of previous research and bioinformatics analysis indicating binding sites for Nrf2 in the FBXL2 promoter and ubiquitination binding sites for FBXL2 in NLRP3, we hypothesized that Scu could alleviate diabetic atherosclerosis through a novel Nrf2-FBXL2-NLRP3 pathway. Specifically, we proposed that Scu activates Nrf2, which upregulates FBXL2 expression, which then promotes NLRP3 ubiquitination and degradation, ultimately inhibiting cellular pyroptosis in the context of diabetic atherosclerosis.

Methods

Cell culture

Human umbilical vein endothelial cells (HUVECs) were obtained from the American Type Culture Collection (ATCC, Manassas, VA, USA; catalog number: PCS-100-010). The cells were cultured in Dulbecco's modified Eagle's medium (DMEM; Gibco, Thermo Fisher Scientific, Waltham, MA, USA) supplemented with 1% endothelial cell growth factor (ECGF; Sigma-Aldrich, St. Louis, MO, USA), 10% fetal bovine serum, and 1% penicillin/streptomycin. The cells were maintained at 37°C in a 5% CO_2 humidified atmosphere. HUVECs between passages 3 and 7 were used for all experiments. Cell identity was confirmed by morphological assessment and expression of endothelial cell markers (CD31 and VE-cadherin). To establish an *in vitro* diabetic atherosclerosis model, HUVECs were treated with different concentrations of glucose. The cells were divided into three groups: the normal glucose (control) group, the negative control (NC) group, and the high glucose (HG) group. The control group was exposed to medium containing 5.5 mM glucose, the NC group received 5.5 mM glucose and 27.5 mM mannitol to control osmotic pressure, and the HG group was supplemented with 33 mM glucose. To investigate the effects of Scu (purity ≥98%, Sigma-Aldrich), HUVECs in the HG group were treated with different concentrations of Scu (5 μM, 10 μM, and 20 μM) for various durations (0 hours, 12 hours, 24 hours, and 48 hours). The optimal concentration of Scu was determined for subsequent experiments.

Cell transfection

For the generation of overexpression or knockdown models *in vitro*, vectors for FBXL2 overexpression (OE-FBXL2), Nrf2 overexpression (OE-Nrf2), Nrf2 knockdown (sh-Nrf2), FBXL2 knockdown (sh-FBXL2), and NLRP3 knockdown (sh-NLRP3) were obtained from Genechem Technology (Shanghai, China). The vectors were transfected with Lipofectamine™ 3000 according to the manufacturer's instructions (Invitrogen, Carlsbad, CA, USA). Briefly, HUVECs were seeded in 6-well plates at a density of 2×10^5 cells/well and cultured to 70–80% confluence. For each well, 2.5 μg of plasmid DNA was diluted in 125 μL of Opti-MEM (Gibco) and mixed with 5 μL of P3000 reagent. In a separate tube, 5 μL of Lipofectamine 3000 was diluted in 125 μL of Opti-MEM. The two solutions were combined, gently mixed, and incubated for 15 minutes at room temperature. The transfection mixture was then added dropwise to the cells. Transfection efficiency was assessed 48 hours posttransfection by fluorescence microscopy to visualize the GFP-tagged constructs and confirmed by qRT-PCR and western blot analysis of target gene expression. Typically, transfection efficiencies ranging from 70–80% were achieved. For proteasome inhibition experiments, cells were treated with MG132 (30 μM; Sigma-Aldrich) for 6 hours. To activate NLRP3, the cells were treated with the NLRP3 activator BMS-986299 (10 μM; MedChemExpress, Monmouth Junction, NJ, USA) for 6 hours. Subsequent experiments were conducted after an additional 48-hour incubation period.

MTT assay

Cell viability was assessed with the MTT assay (Solarbio, Beijing, China). Human umbilical vein endothelial cells (HUVECs) were seeded in 96-well plates at a density of 5×10^3 cells per well and allowed to adhere overnight. After treating the cells under different conditions, the culture medium was replaced with 20 μL of MTT solution (5 mg/mL) in each well. The cells were incubated for 4 hours at 37°C to allow the conversion of MTT into formazan crystals. Then, 150 μL of dimethyl sulfoxide (DMSO) was added to dissolve the formazan crystals. The absorbance was measured at 490 nm using a microplate reader. Cell viability was calculated as the percentage of absorbance in the treated cells compared with the control cells.

Lactate dehydrogenase (LDH) assay

Cellular cytotoxicity was determined by measuring the release of LDH using an LDH assay kit (Solarbio, Beijing, China). HUVECs were seeded in 96-well plates at a density of 5×10^3 cells per well and cultured for 24 hours. After the cells were subjected to different conditions, the culture supernatant was collected, and LDH activity was measured following the manufacturer's instructions. Briefly, 50 μL of the culture supernatant was mixed with 50 μL of the provided reaction solution in the kit. The mixture was incubated at room temperature for 30 minutes, and the reaction was stopped by adding 50 μL of stop solution. The absorbance was measured at 490 nm using a microplate reader. LDH release was normalized to that of the control group.

Hoechst 33342/PI double staining

To evaluate the occurrence of pyroptosis, Hoechst 33342/PI double staining (Sigma-Aldrich, St. Louis, MO, USA) was performed. After treating HUVECs under various conditions, the cells were washed with phosphate-buffered saline and then stained with Hoechst 33342 dye for 10 minutes at 37°C in the dark. The cells were subsequently incubated with propidium iodide (PI) for 5 minutes at room temperature. The stained cells were observed under a fluorescence microscope (Olympus, Tokyo, Japan). Pyroptotic cells were identified by the presence of condensed and fragmented nuclei stained with Hoechst 33342, as well as the uptake of PI, which indicated the loss of plasma membrane integrity.

ELISA

To quantify the expression levels of inflammatory cytokines, including TNF-α, IL-1β and IL-18, in the culture supernatant, ELISAs were performed. The culture supernatant was collected and centrifuged to remove cellular debris. The levels of TNF-α, IL-1β, and IL-18 were measured with specific ELISA kits (Beyotime, Shanghai, China) according to the manufacturer's instructions. Then, we constructed standard curves for TNF-α, IL-1β, and IL-18, as detailed in Supplementary Figs. 1, 2.

Dual-luciferase reporter assay

To investigate the effect of Nrf2 on the activity of the FBXL2 promoter, a potential binding site was predicted with the bioinformatics tool JASPAR. The corresponding regions, which included the wild-type FBXL2 promoter (WT-FBXL2) and the mutant FBXL2 promoter (MUT-FBXL2), were amplified by PCR and cloned and inserted into the pGL4 vector (Promega, Madison, WI, USA). Cotransfection experiments were performed by cotransfecting Nrf2 overexpression vectors along with the cloned pGL4 vector with Lipofectamine 3000 (Invitrogen, Carlsbad, CA, USA) according to the manufacturer's instructions. After 24 hours of transfection, luciferase activity was measured with a dual-luciferase reporter system (Promega, Madison, WI, USA). The relative luciferase activity was determined by calculating the ratio of firefly luciferase activity to Renilla luciferase activity.

Immunoprecipitation (IP)

To assess the level of ubiquitinated NLRP3, IP was performed. Briefly, the cell lysates were incubated with antibodies against NLRP3 (ab263899, Abcam, 1:1,000) and ubiquitin (ab134953, Abcam, 1:1,000) overnight at 4°C. Protein A/G agarose beads were then added to capture the antibody-protein complexes. After incubation, the beads were washed to remove nonspecifically bound proteins. The immunoprecipitated proteins were eluted from the beads, separated by SDS-PAGE, and analyzed by immunoblot analysis as previously described [17].

Western blotting

The cells were lysed with RIPA buffer (Bocai, Shanghai, China) supplemented with protease and phosphatase inhibitors. The protein lysates were quantified with a BCA protein assay kit (Beyotime, Shanghai, China). Equal amounts of protein were separated by SDS-PAGE and transferred onto PVDF membranes (Millipore, MA, USA). The membrane was blocked with 5% nonfat milk and incubated overnight at 4°C with primary antibodies specific for Nrf2 (ab62352, Abcam, 1:1,000), FBXL2 (ab153842, Abcam, 1:1,000), NLRP3 (ab263899, Abcam, 1:1,000), cleaved caspase-1 (D57A2, Cell Signaling, 1:1,000), and β-actin (ab8226, Abcam, 1:1,000). After washing, the membrane was incubated with secondary antibodies (ab202901, Abcam, 1:1,000) conjugated to horseradish peroxidase (HRP) for 1 hour at room temperature. The protein bands were visualized, the band intensities were quantified with ImageJ software, and the protein expression levels were normalized to that of β-actin, which was used as an internal control.

Statistical analysis

All the statistical analyses were performed with GraphPad Prism version 7.0 (GraphPad Software, San Diego, CA, USA). The data are presented as the means ± standard deviations (SDs). The number of biological replicates (*n*) for each experiment is indicated in the corresponding figure legends. Prior to analysis, the data were tested for normality by the *Shapiro-Wilk test* and for homogeneity of variance by *Levene's test*. For comparisons between two groups, two-tailed unpaired *Student's t tests* were used when the data were normally distributed. For comparisons involving more than two groups, one-way analysis of variance (*ANOVA*) was used

for normally distributed data with homogeneous variances, followed by *Tukey's honest significant difference (HSD) test* for post hoc pairwise comparisons. For all the statistical tests, a p value less than 0.05 was considered statistically significant. Specific p values are reported in the figure legends, with the following notations: $*p < 0.05$, $**p < 0.01$, $***p < 0.001$, and $****p < 0.0001$. Nonsignificant differences are indicated as 'ns.' Sample size estimation and power analysis were conducted with G*Power 3.1 software to ensure adequate sample sizes for detecting biologically meaningful effects, with a power of 0.8 and an alpha level of 0.05. For the cell culture experiments, each independent experiment was performed in triplicate, and a minimum of three independent experiments were conducted to ensure adequate statistical power.

Results

HG treatment decreased Nrf2 and FBXL2 levels and promoted NLRP3-mediated pyroptosis

As shown in Supplementary Fig. 3, as the glucose concentration increased, the cell viability decreased. In addition, cell viability was significantly lower in the HG group than in the control and NC groups in a time-dependent manner (Fig. 1A). Western blot analysis (Fig. 1B) revealed that Nrf2 and FBXL2 expression was downregulated, while NLRP3 and cleaved caspase-1 expression was upregulated upon HG treatment. Additionally, LDH release was markedly increased in the HG group, indicating the induction of cytotoxicity by HG (Fig. 1C). Hoechst 33342/PI double staining revealed increased pyroptosis in response to HG treatment compared with that in the control and NC groups (Fig. 1D). Furthermore, the ELISAs confirmed the upregulation of proinflammatory cytokines, including IL-18, TNF-α, and IL-1β, upon HG treatment (Fig. 1E). In all of the aforementioned experiments, no significant difference was observed between the NC group and the control group, which suggested that the osmotic pressure had no discernible effect. Collectively, these findings suggest that HG treatment suppresses Nrf2 and FBXL2 expression while promoting NLRP3-mediated pyroptosis and inflammation.

Scu enhanced Nrf2 expression, improved cell viability and inhibited pyroptosis

The effects of Scu on cellular responses were investigated with different concentrations of Scu and various treatment durations. As depicted in Fig. 2A, Scu treatment resulted in a dose-dependent and time-dependent increase in cell viability compared with that of the HG group. Moreover, Scu treatment partially reversed the HG-induced decrease in Nrf2 levels (Fig. 2B) and attenuated HG-induced cytotoxicity (Fig. 2C). In addition, Scu treatment inhibited pyroptosis in the HG + Scu groups compared with that in the HG group (Fig. 2D). Furthermore, the addition of Scu to the HG culture medium led to a reduction in the levels of proinflammatory cytokines, including IL-18, TNF-α, and IL-1β (Fig. 2E). These findings suggest that Scu may increase Nrf2 expression and ameliorate symptoms of diabetic atherosclerosis.

Depletion of Nrf2 downregulated FBXL2 and reversed the protective effects of Scu

The binding site of transcription factor Nrf2 in the FBXL2 promoter was predicted by the JASPAR website (https://jaspar.genereg.net/). Using a dual-luciferase assay to examine the binding relationship between Nrf2 and the FBXL2 promoter. The dual-luciferase reporter assay further revealed potential binding interactions between Nrf2 and FBXL2 (Fig. 3A). To further understand the relationships among Scu, Nrf2, and FBXL2, we established an Nrf2 knockdown model and an FBXL2 overexpression model. Western blot analysis revealed that sh-Nrf2 decreased the protein levels of Nrf2 and FBXL2, whereas transfection with OE-FBXL2 increased FBXL2 expression without affecting Nrf2 levels (Fig. 3B). In the HG + Scu + sh-Nrf2 group, cell viability was significantly lower than that in the HG + Scu group. However, the overexpression of FBXL2 counteracted the effects of Nrf2 knockdown, leading to increased cell viability (Fig. 3C). In the HG + Scu + sh-Nrf2 group, pyroptosis (Fig. 3D) and the levels of proinflammatory cytokines (Fig. 3E) were increased. These findings suggest that Scu exerts its protective effects on diabetic atherosclerosis through the Nrf2 pathway and its downstream gene FBXL2.

FBXL2 promoted the ubiquitination-mediated degradation of NLRP3 and inhibited pyroptosis

To elucidate the underlying molecular mechanism, MG132, a protease inhibitor, was used. FBXL2 downregulated NLRP3 expression, but the addition of MG132 abrogated the inhibitory effects of FBXL2 on NLRP3 levels (Fig. 4A). Immunoprecipitation further confirmed that the downregulation of NLRP3 by FBXL2 was dependent on protease activity (Fig. 4B). Notably, the protein level of FBXL2 was decreased, whereas the levels of NLRP3 and cleaved caspase-1 were increased in the HG + Scu + sh-FBXL2 group compared with those in the HG + Scu group (Fig. 4C). Depletion of FBXL2 inhibited cell viability (Fig. 4D) and enhanced cytotoxicity (Fig. 4E). Additionally, sh-FBXL2 transfection promoted pyroptosis (Fig. 4F), and the proinflammatory

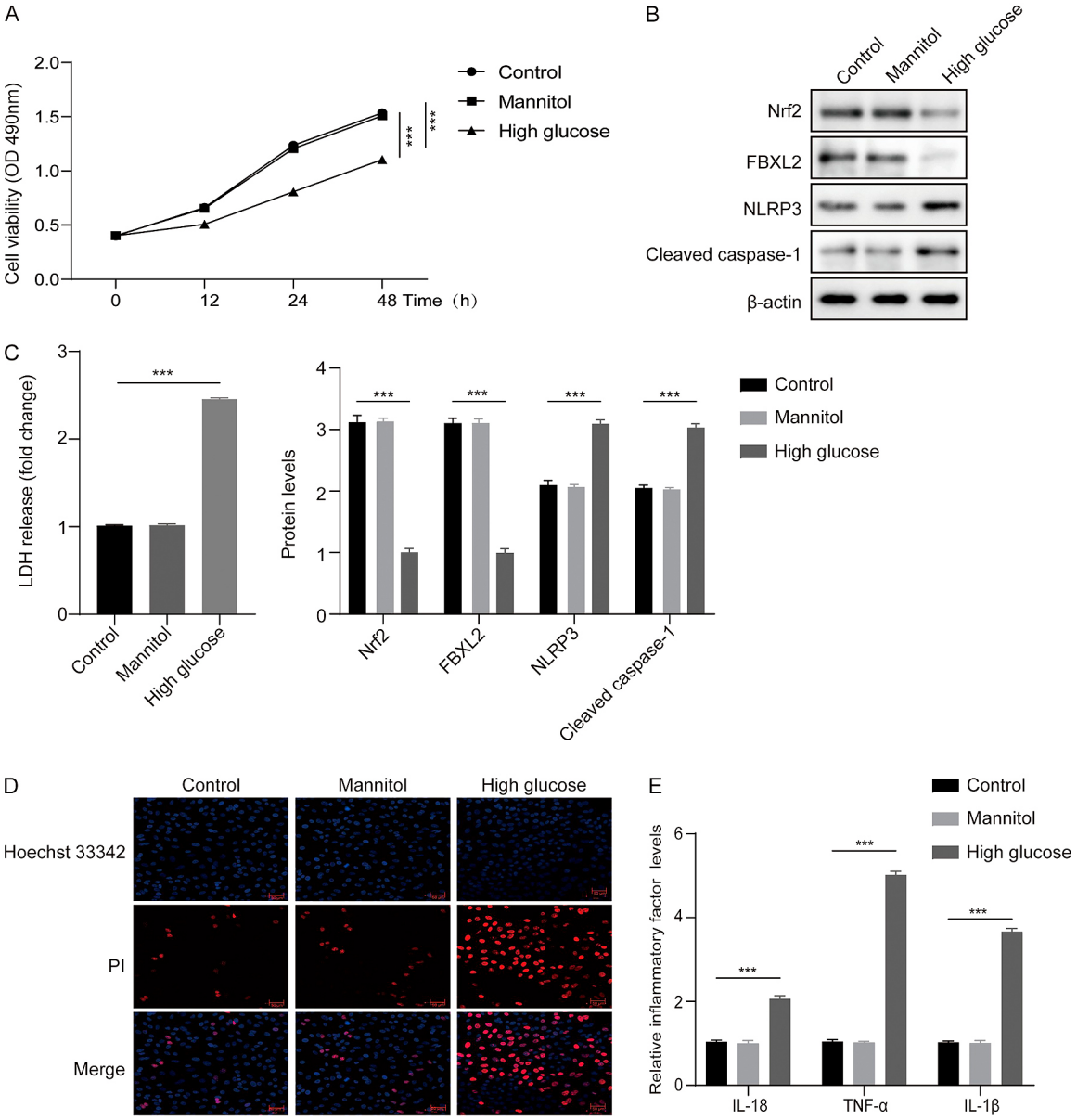

Fig. 1 HG treatment decreased Nrf2 and FBXL2 levels, increased NLRP3 expression and promoted pyroptosis. (A) Cell viability was determined by the MTT assay. (B) The protein expression of Nrf2, FBXL2, NLRP3 and cleaved caspase-1 was assessed by western blotting. (C) Cell cytotoxicity was evaluated by LDH assay. (D) Cell pyroptosis was monitored by Hoechst 33342/PI double staining. (E) The levels of the proinflammatory cytokines IL-18, TNF-α, and IL-1β were measured by ELISA. ***$p <$ 0.001.

cytokines IL-18, TNF-α, and IL-1β were upregulated upon FBXL2 knockdown (Fig. 4G). These data highlight the role of FBXL2 in facilitating the ubiquitination-mediated degradation of NLRP3, which contributes to the amelioration of diabetic atherosclerosis symptoms.

Activation of NLRP3 reversed the protective effects of Scu on diabetic atherosclerosis

To further investigate the relationship between NLRP3 and the Nrf2-FBXL2 axis, we manipulated NLRP3 expression with sh-NLRP3 or the NLRP3 activator BMS-986299 in the HG + Scu + sh-Nrf2 group. As depicted in Fig. 5A, depletion of NLRP3 reversed the inhibitory effects of sh-Nrf2 on FBXL2 and NLRP3 expression. Cell viability was increased in cells transfected with sh-NLRP3 compared to those transfected with sh-Nrf2, whereas treatment with the NLRP3 activator reduced cell viability (Fig. 5B). Furthermore, depletion of NLRP3 significantly reduced cell cytotoxicity (Fig. 5C) and pyroptosis (Fig. 5D). This depletion effectively reversed the effects caused by Nrf2 depletion. Interestingly, the activation of NLRP3 presented synergistic effects with the inhibition

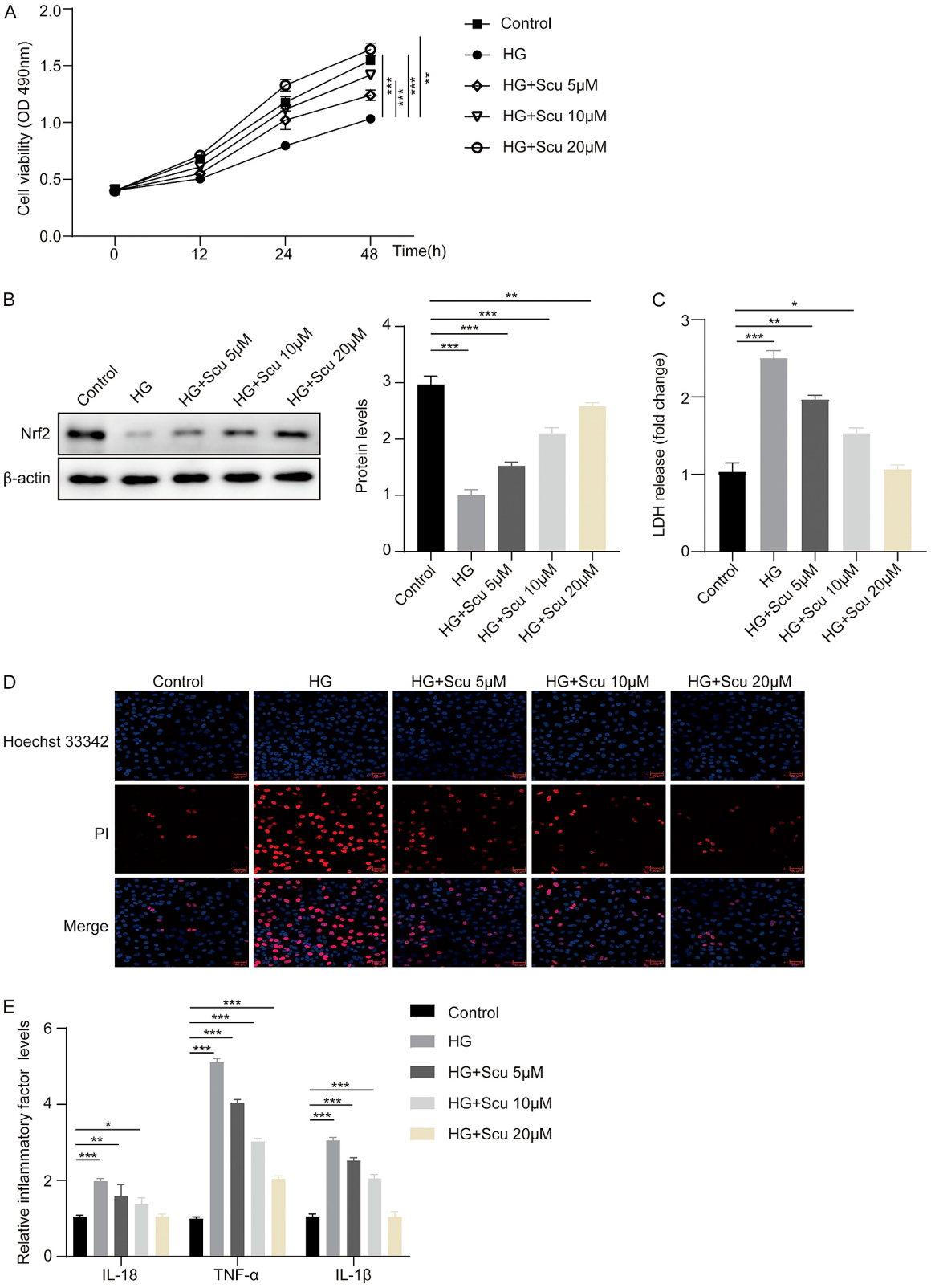

Fig. 2 Scu enhanced Nrf2 expression, improved cell viability and inhibited pyroptosis. (A) Cell viability was determined by the MTT assay. (B) The protein expression of Nrf2 was assessed by western blotting. (C) Cell cytotoxicity was evaluated by LDH assay. (D) Cell pyroptosis was monitored by Hoechst 33342/PI double staining. (E) The levels of the proinflammatory cytokines IL-18, TNF-α, and IL-1β were measured by ELISA. *$p < 0.05$, **$p < 0.01$, ***$p < 0.001$.

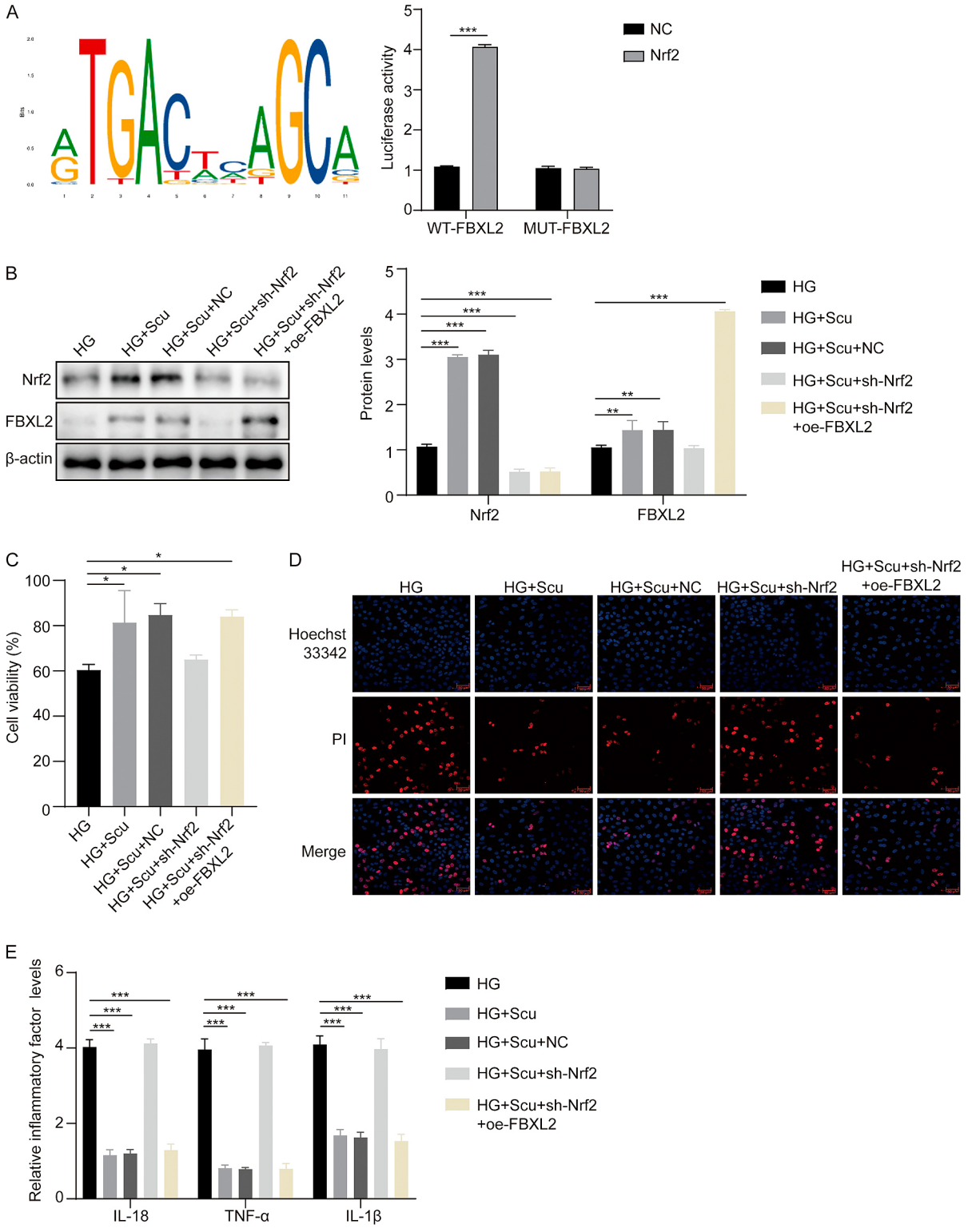

Fig. 3 Depletion of Nrf2 downregulated FBXL2 and reversed the protective effects of Scu. (A) The potential binding relationship between Nrf2 and FBXL2 was verified by a dual-luciferase reporter assay. (B) The protein expression of Nrf2 and FBXL2 was assessed by western blotting. (C) Cell viability was determined by the MTT assay. (D) Cell pyroptosis was monitored by Hoechst 33342/PI double staining. (E) The levels of the proinflammatory cytokines IL-18, TNF-α, and IL-1β were measured by ELISA. $^{*}p < 0.05$, $^{**}p < 0.01$, $^{***}p < 0.001$.

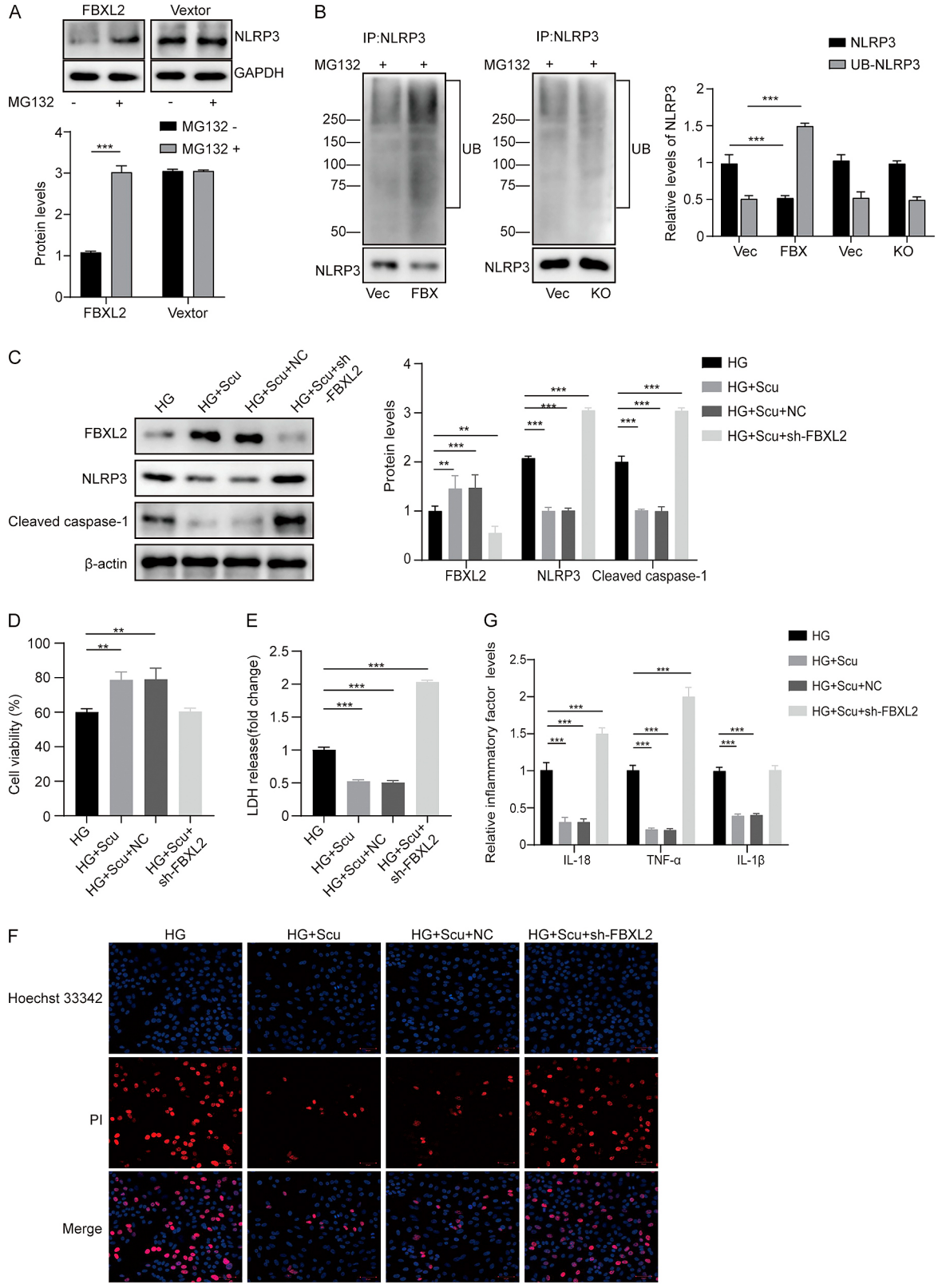

Fig. 4 FBXL2 promoted the ubiquitination-mediated degradation of NLRP3 and inhibited pyroptosis. (A) Protein expression of NLRP3 was assessed by western blotting. (B) NLRP3 ubiquitination was determined by western blotting. (C) The protein expression of FBXL2, NLRP3 and cleaved caspase-1 was assessed by western blotting. (D) Cell viability was determined by the MTT assay. (E) Cell cytotoxicity was evaluated by LDH assay. (F) Cell pyroptosis was monitored by Hoechst 33342/PI double staining. (G) The levels of the proinflammatory cytokines IL-18, TNF-α, and IL-1β were measured by ELISA. $^{**}p < 0.01$, $^{***}p < 0.001$.

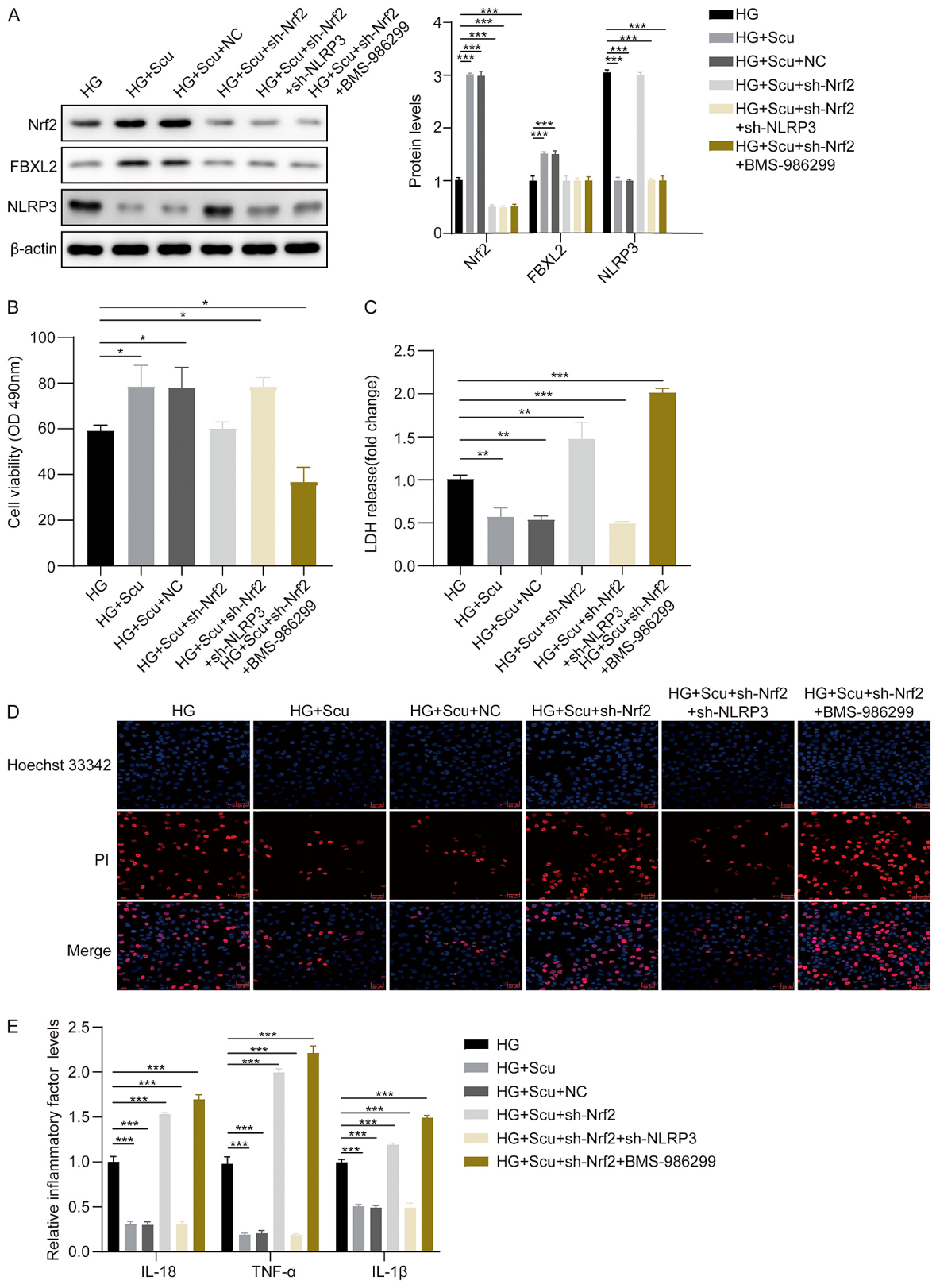

Fig. 5 Depletion of NLRP3 reversed the protective effects of Scu on diabetic atherosclerosis mediated by the Nrf2-FBXL2 axis. (A) The protein expression of Nrf2, FBXL2, and NLRP3 was assessed by western blotting. (B) Cell viability was determined by the MTT assay. (C) Cell cytotoxicity was evaluated by LDH assay. (D) Cell pyroptosis was monitored by Hoechst 33342/PI double staining. (E) The levels of the proinflammatory cytokines IL-18, TNF-α, and IL-1β were measured by ELISA. *$p < 0.05$, **$p < 0.01$, ***$p < 0.001$.

of Nrf2, resulting in increased cytotoxicity and pyroptosis. Importantly, knockdown of NLRP3 reversed the increased expression of the proinflammatory cytokines IL-18, TNF-α, and IL-1β induced by sh-Nrf2. The combined use of sh-Nrf2 and BMS-986299 (NLRP3 agonist for the activation of the NLRP3 inflammasome) had synergistic effects on cell inflammation (Fig. 5E). Collectively, these results indicate that Scu attenuates diabetic atherosclerosis through the upregulation of Nrf2-mediated FBXL2 and the promotion of ubiquitination-mediated degradation of NLRP3.

Discussion

The effects of Scu, a bioactive compound, have been extensively investigated for their role in alleviating various diabetic complications. In diabetic cardiomyopathy, Scu has been shown to reduce proinflammatory cytokine levels and enhance antioxidant enzyme activities, thereby suppressing NLRP3/NF-κB signaling activation and alleviating diabetic cardiomyopathy symptoms in STZ-induced mouse models [18]. Li *et al.* demonstrated that Scu treatment downregulated IL-1β and IL-18 levels, inhibited the expression of NLRP3, GSDMD, and cleaved caspase-1, and reduced pyroptosis in diabetic retinopathy model mice, highlighting its potential therapeutic application in diabetic retinopathy [19]. Moreover, through oral administration, Scu has been found to attenuate elevated total cholesterol levels in serum induced by an atherogenic diet and decrease the atherogenic index [20]. The present study revealed that Scu treatment significantly increased cell viability, inhibited inflammation and suppressed pyroptosis in diabetic atherosclerosis. Therefore, we subsequently investigated the effects of Scu on Nrf2 and FBXL2 to explore the comprehensive mechanisms involved.

Pyroptosis has emerged as a crucial process involved in the pathogenesis of various diseases, as it triggers inflammatory responses and cell membrane rupture through the activation of gasdermin proteins [21]. Recent research has revealed that METTL14-mediated downregulation of TINCR lncRNA decreases NLRP3 stability and pyroptosis, resulting in the attenuation of diabetic cardiomyopathy [22]. The activation of inflammasome pathways has also been associated with increased pyroptosis in diabetic kidney disease [23]. In the context of diabetic atherosclerosis, Zhu *et al.* demonstrated that salvianolic acid A inhibited PKR phosphorylation and suppressed NLRP3 inflammasome-mediated pyroptosis in endothelial cells [24]. Similarly, we observed increased pyroptosis and NLRP3 expression in HG-treated cells, and depletion of NLRP3 attenuated the progression of diabetic atherosclerosis, underscoring the therapeutic potential of targeting pyroptosis pathways in the management of diabetic atherosclerosis.

Nrf2, a transcription factor known for its involvement in cellular antioxidant and anti-inflammatory responses, has been implicated in the development of atherosclerosis in diabetes. Huang *et al.* demonstrated that Nrf2 improved endothelial function by mitigating oxidative stress and mitochondrial damage, thereby delaying the progression of atherosclerosis [25]. Additionally, Nrf2 was found to regulate the phenotype of vascular smooth muscle cells, inhibiting processes such as calcification and apoptosis and thereby alleviating atherosclerosis [26]. Consistent with these findings, our experimental results support the role of Nrf2 in the inhibition of atherosclerosis in diabetes through Scu-induced upregulation of Nrf2 expression.

FBXL2 belongs to an E3 ubiquitin ligase subunit and can mediate the degradation of various proteins [27, 28]. Previous research has shown that FBXL2 interacts with the mitophagy protein FUNDC1, leading to the degradation of IP3R3 [29]. In this study, for the first time, we revealed the interaction between Nrf2 and FBXL2 and demonstrated that Nrf2-upregulated FBXL2 contributes to the ubiquitination-mediated degradation of NLRP3. Furthermore, Jeon *et al.* highlighted the role of FBXL2-mediated ubiquitination and degradation of NLRP3 in promoting inflammation-related diseases [30]. Our results revealed that depletion of FBXL2 increased NLRP3 levels, whereas overexpression of FBXL2 suppressed pyroptosis and alleviated the inflammatory state. Although our study revealed the upregulation of Nrf2 and FBXL2 by Scu, the precise molecular mechanisms involved warrant further investigation. Scu may modify the negative regulator of Nrf2, influence epigenetic modifications at the Nrf2 gene locus, or downregulate miRNAs that target Nrf2 mRNA. Additionally, Scu might influence FBXL2 expression through other transcription factors or signaling pathways that work in concert with or independently of Nrf2. Elucidating these mechanisms would provide a more comprehensive understanding of the effects of Scu on diabetic atherosclerosis and potentially reveal new therapeutic targets.

Our findings on the protective effects of Scu in diabetic atherosclerosis align with and extend recent advances in the field. The study by Tong *et al.* on the sensitive detection of intraplaque hemorrhage highlights the need for advanced monitoring of atherosclerosis progression, which could be valuable in future assessments of Scu efficacy [31]. Our focus on NLRP3 regulation by Scu is supported by recent proteomic studies that emphasized the importance of inflammatory markers in cardiovascular outcomes [32]. The distinct metabolic features of type 2 diabetes and coronary artery disease identified by Smith

et al. underscore the relevance of our targeted approach to the Nrf2 and FBXL2 pathways [33]. These recent findings collectively reinforce the complexity of diabetic atherosclerosis and highlight the potential of Scu as a multifaceted therapeutic agent that acts through NLRP3 degradation and Nrf2 activation while also suggesting new avenues for investigation to fully elucidate its therapeutic potential.

In conclusion, our *in vitro* study demonstrated that Scu attenuates high glucose-induced endothelial cell dysfunction, a key feature of diabetic atherosclerosis. Our data revealed that Scu enhances Nrf2 expression in high glucose-treated HUVECs, leading to increased FBXL2 expression, which promotes NLRP3 ubiquitination and subsequent degradation, ultimately reducing pyroptosis in endothelial cells (Graphical Abstract). These findings suggest a novel mechanism by which Scu may protect against endothelial dysfunction in the context of diabetic atherosclerosis. However, several limitations should be considered, including the exclusive use of *in vitro* models, the lack of direct atherosclerotic plaque measurements, and the focus on a single cell type. Future research should address these limitations through *in vivo* studies, investigations of other cell types involved in atherosclerosis, and clinical studies to assess the safety and efficacy of Scu in patients. Ji *et al.* demonstrated that β-OHB alleviated myocardial oxidative stress and improved mitochondrial function through the FoxO3a/MT2 antioxidant pathway in a sepsis model. Future research could explore the potential synergistic effects of Scu and ketone bodies such as β-OHB in treating diabetic atherosclerosis and investigate whether Scu influences pathways similar to those of β-OHB [34]. The hyperglycemic conditions used in our study were higher than typical clinical levels and were selected to model severe glucose stress in individuals with diabetes. While this model provides valuable insights, it may not fully reflect the chronic, moderate hyperglycemia observed in patients. Future studies using more clinically relevant glucose concentrations and *in vivo* models are needed to confirm the clinical applicability of scutellarin. While our results provide a promising foundation for understanding the molecular mechanisms of Scu in diabetic atherosclerosis, further research is needed to fully elucidate its therapeutic potential and translate these findings into clinical applications.

Declarations

Funding

This study was supported by Professor and Doctoral Research Project at Changsha Social Work College (No. 2024JB28, No. 2024JB29), The Research Fund Project

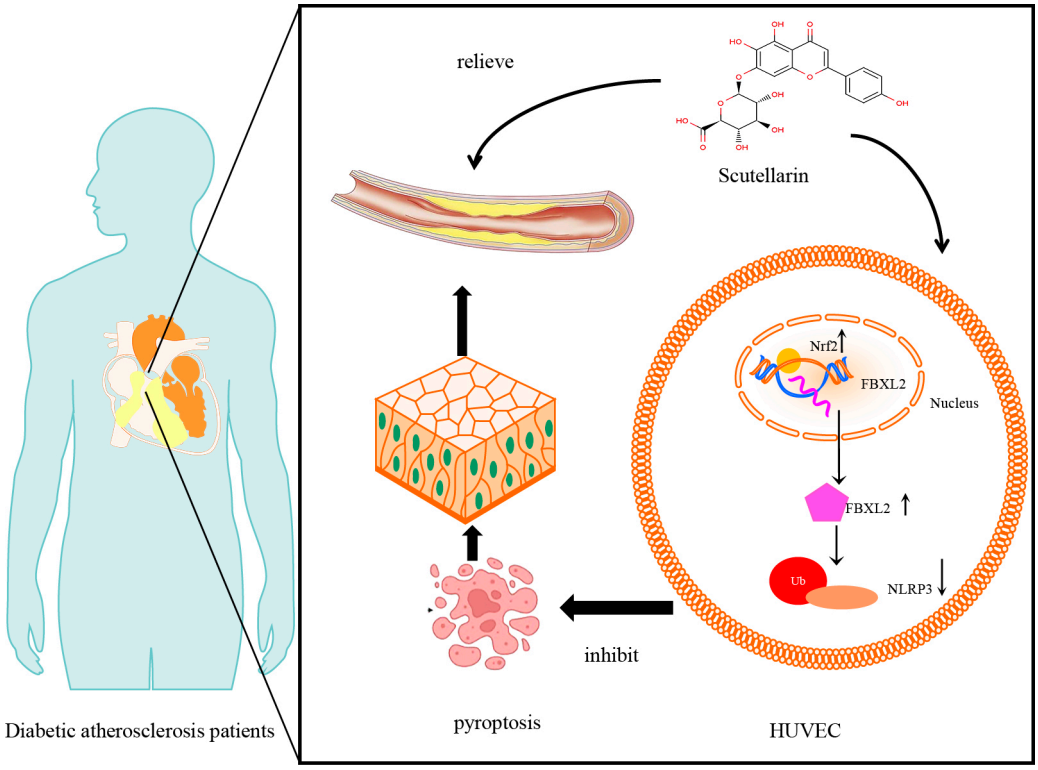

Graphical Abstract Scutellarin alleviated diabetic atherosclerosis by enhancing Nrf2 and FBXL2 expression, which further promoted the ubiquitination-mediated degradation of NLRP3 and suppressed cell pyroptosis.

of Hunan Provincial Department of Education (No. 22C1424, No. 23B1113) and Natural Science Foundation of Hunan Province (No. 2025JJ80321).

Conflict of interest

The authors declare that they have no competing interests.

Acknowledgements

Not applicable.

Ethics approval

Not applicable.

Availability of data and material

All data generated or analyzed during this study are available on request to the corresponding author.

Authors' contributions

Guarantor of integrity of the entire study: Qingxin Meng

Study concepts: Qingxin Meng

Study design: Qingxin Meng, Yongpan Huang

Definition of intellectual content: Qingxin Meng, Xian Long

Literature research: Qingxin Meng, Lijing Liu

Clinical studies: Yani Tang, Yayuan Luo

Experimental studies: Qingxin Meng, Yayuan Luo, Xian Long

Data acquisition: Qingxin Meng, Yongpan Huang

Data analysis: Qingxin Meng, Jingjing He

Statistical analysis: Qingxin Meng, Jingjing He

Manuscript preparation: Qingxin Meng, Yani Tang

Manuscript editing: Yongpan Huang, Xian Long

Manuscript review: Yongpan Huang, Lijing Liu

All authors have read and approved the final version of this manuscript to be published.

References

1. Kong P, Cui ZY, Huang XF, Zhang DD, Guo RJ, *et al.* (2022) Inflammation and atherosclerosis: signaling pathways and therapeutic intervention. *Signal Transduct Target Ther* 7: 131.
2. Xiang Q, Tian F, Xu J, Du X, Zhang S, *et al.* (2022) New insight into dyslipidemia-induced cellular senescence in atherosclerosis. *Biol Rev Camb Philos Soc* 97: 1844–1867.
3. Peng J, Luo F, Ruan G, Peng R, Li X (2017) Hypertriglyceridemia and atherosclerosis. *Lipids Health Dis* 16: 233.
4. Poznyak AV, Bharadwaj D, Prasad G, Grechko AV, Sazonova MA, *et al.* (2021) Renin-angiotensin system in pathogenesis of atherosclerosis and treatment of CVD. *Int J Mol Sci* 22: 6702.
5. Wu X, Zhang H, Qi W, Zhang Y, Li J, *et al.* (2018) Nicotine promotes atherosclerosis *via* ROS-NLRP3-mediated endothelial cell pyroptosis. *Cell Death Dis* 9: 171.
6. Peng L, Wen L, Shi QF, Gao F, Huang B, *et al.* (2020) Scutellarin ameliorates pulmonary fibrosis through inhibiting NF-κB/NLRP3-mediated epithelial-mesenchymal transition and inflammation. *Cell Death Dis* 11: 978.
7. Zhang Q, Liu J, Duan H, Li R, Peng W, *et al.* (2021) Activation of Nrf2/HO-1 signaling: an important molecular mechanism of herbal medicine in the treatment of atherosclerosis *via* the protection of vascular endothelial cells from oxidative stress. *J Adv Res* 34: 43–63.
8. Deng M, Sun J, Peng L, Huang Y, Jiang W, *et al.* (2022) Scutellarin acts on the AR-NOX axis to remediate oxidative stress injury in a mouse model of cerebral ischemia/reperfusion injury. *Phytomedicine* 103: 154214.
9. Liu Y, Uruno A, Saito R, Matsukawa N, Hishinuma E, *et al.* (2022) Nrf2 deficiency deteriorates diabetic kidney disease in Akita model mice. *Redox Biol* 58: 102525.
10. Yamamoto M, Kensler TW, Motohashi H (2018) The KEAP1-NRF2 system: a thiol-based sensor-effector apparatus for maintaining redox homeostasis. *Physiol Rev* 98: 1169–1203.
11. Linna-Kuosmanen S, Tomas Bosch V, Moreau PR, Bouvy-Liivrand M, Niskanen H, *et al.* (2021) NRF2 is a key regulator of endothelial microRNA expression under proatherogenic stimuli. *Cardiovasc Res* 117: 1339–1357.
12. Wu H, Jia L (2019) Scutellarin attenuates hypoxia/reoxygenation injury in hepatocytes by inhibiting apoptosis and oxidative stress through regulating Keap1/Nrf2/ARE signaling. *Biosci Rep* 39: BSR20192501.
13. Niu M, Xu J, Liu Y, Li Y, He T, *et al.* (2021) FBXL2 counteracts Grp94 to destabilize EGFR and inhibit EGFR-driven NSCLC growth. *Nat Commun* 12: 5919.
14. Humphries F, Bergin R, Jackson R, Delagic N, Wang B, *et al.* (2018) The E3 ubiquitin ligase Pellino2 mediates priming of the NLRP3 inflammasome. *Nat Commun* 9: 1560.
15. Chen X, Liu G, Yuan Y, Wu G, Wang S, *et al.* (2019) NEK7 interacts with NLRP3 to modulate the pyroptosis in inflammatory bowel disease *via* NF-κB signaling. *Cell Death Dis* 10: 906.
16. Sun L, Ma W, Gao W, Xing Y, Chen L, *et al.* (2019) Propofol directly induces caspase-1-dependent macrophage pyroptosis through the NLRP3-ASC inflammasome. *Cell Death Dis* 10: 542.
17. Han S, Lear TB, Jerome JA, Rajbhandari S, Snavely CA, *et al.* (2015) Lipopolysaccharide primes the NALP3 inflammasome by inhibiting its ubiquitination and degradation mediated by the SCFFBXL2 E3 ligase. *J Biol Chem* 290: 18124–18133.

18. Xu L, Chen R, Zhang X, Zhu Y, Ma X, *et al.* (2021) Scutellarin protects against diabetic cardiomyopathy *via* inhibiting oxidative stress and inflammatory response in mice. *Ann Palliat Med* 10: 2481–2493.
19. Li N, Guo XL, Xu M, Chen JL, Wang YF, *et al.* (2023) Network pharmacology mechanism of Scutellarin to inhibit RGC pyroptosis in diabetic retinopathy. *Sci Rep* 13: 6504.
20. Li Q, Wu JH, Guo DJ, Cheng HL, Chen SL, *et al.* (2009) Suppression of diet-induced hypercholesterolemia by scutellarin in rats. *Planta Med* 75: 1203–1208.
21. Zuo Y, Chen L, Gu H, He X, Ye Z, *et al.* (2021) GSDMD-mediated pyroptosis: a critical mechanism of diabetic nephropathy. *Expert Rev Mol Med* 23: e23.
22. Meng L, Lin H, Huang X, Weng J, Peng F, *et al.* (2022) METTL14 suppresses pyroptosis and diabetic cardiomyopathy by downregulating TINCR lncRNA. *Cell Death Dis* 13: 38.
23. Liu P, Zhang Z, Li Y (2021) Relevance of the pyroptosis-related inflammasome pathway in the pathogenesis of diabetic kidney disease. *Front Immunol* 12: 603416.
24. Zhu J, Chen H, Le Y, Guo J, Liu Z, *et al.* (2022) Salvianolic acid A regulates pyroptosis of endothelial cells *via* directly targeting PKM2 and ameliorates diabetic atherosclerosis. *Front Pharmacol* 13: 1009229.
25. Huang Z, Wu M, Zeng L, Wang D (2022) The beneficial role of Nrf2 in the endothelial dysfunction of atherosclerosis. *Cardiol Res Pract* 2022: 4287711.
26. Zhuang W, Yang Y, Li H, Liang J (2021) Research advance of Nrf2 on atherosclerosis by regulating vascular smooth muscle cell. *Zhejiang Da Xue Xue Bao Yi Xue Ban* 50: 390–395.
27. Chen BB, Glasser JR, Coon TA, Mallampalli RK (2011) FBXL2 is a ubiquitin E3 ligase subunit that triggers mitotic arrest. *Cell Cycle* 10: 3487–3494.
28. Das A, Wang X, Wei J, Hoji A, Coon TA, *et al.* (2022) Cross-regulation of F-box protein FBXL2 with T-bet and TNF-α during acute and chronic lung allograft rejection. *J Immunol* 209: 1788–1795.
29. Ren J, Sun M, Zhou H, Ajoolabady A, Zhou Y, *et al.* (2020) FUNDC1 interacts with FBXL2 to govern mitochondrial integrity and cardiac function through an IP3R3-dependent manner in obesity. *Sci Adv* 6: eabc8561.
30. Jeon S, Kang J, Lee SB (2023) BC-1215 inhibits ATP-induced IL-1β secretion *via* the FBXL2-mediated ubiquitination and degradation of not only NLRP3, but also pro-IL-1β in LPS-primed THP-1 cells. *Biochem Biophys Res Commun* 657: 128–135.
31. Tong W, Zhang Y, Hui H, Feng X, Ning B, *et al.* (2023) Sensitive magnetic particle imaging of haemoglobin degradation for the detection and monitoring of intraplaque haemorrhage in atherosclerosis. *EBioMedicine* 90: 104509.
32. Bakhshi H, Michelhaugh SA, Bruce SA, Seliger SL, Qian X, *et al.* (2023) Association between proteomic biomarkers and myocardial fibrosis measured by MRI: the multi-ethnic study of atherosclerosis. *EBioMedicine* 90: 104490.
33. Smith ML, Bull CJ, Holmes MV, Davey Smith G, Sanderson E, *et al.* (2023) Distinct metabolic features of genetic liability to type 2 diabetes and coronary artery disease: a reverse Mendelian randomization study. *EBioMedicine* 90: 104503.
34. Ji L, He Q, Liu Y, Deng Y, Xie M, *et al.* (2022) Ketone body β-hydroxybutyrate prevents myocardial oxidative stress in septic cardiomyopathy. *Oxid Med Cell Longev* 2022: 2513837.